Journal of Hazardous Materials 165 (2009) 345–352

Contents lists available at ScienceDirect

Journal of Hazardous Materials

journal homepage: www.elsevier.com/locate/jhazmat

Treatment of bio-digester effluent by electrocoagulation using iron electrodes

Mayank Kumar, F. Infant Anto Ponselvan, Jodha Ram Malviya, Vimal Chandra Srivastava, Indra Deo Mall *

Department of Chemical Engineering, Indian Institute of Technology Roorkee, Roorkee 247667, India

A R T I C L E   I N F O

Article history:
Received 12 April 2008
Received in revised form
30 September 2008
Accepted 1 October 2008
Available online 19 October 2008

Keywords:
Electrocoagulation
COD removal
Response surface methodology
Iron electrode
Distillery effluent

A B S T R A C T

The present paper deals with chemical oxygen demand (COD) reduction of a bio-digester effluent (BDE) in a batch electrocoagulation (EC) reactor using iron electrode. A central composite (CC) experimental design has been employed to evaluate the individual and interactive effects of four independent parameters on the COD removal efficiency. The parameters studied are current density (j): 44.65–223.25 A/m^2; initial pH (pH_0): 2–8; inter-electrode distance (g): 1–3 cm and electrolysis time (t): 30–150 min. The results have been analyzed using Pareto analysis of variance (ANOVA). Analysis showed a high coefficient of determination value (R^2 = 0.8547) and satisfactory prediction for second-order regression model. Graphical response surface and contour plots have been used to locate the optimum values of studied parameters. Maximum COD and color reduction of 50.5% and 95.2%, respectively, was observed at optimum conditions. Present study shows that EC technique can be employed in distilleries to reduce the pollution load before treatment in aerobic treatment plants to meet the discharge standards.

1. Introduction

Ethanol manufacture from molasses generates large volumes of high strength wastewater that is of serious environmental concern. India is the second largest producer of ethanol in Asia with around 319 distilleries, producing 3.25×10^9 l of alcohol, and generating 40.4×10^{10} l of wastewater annually [1,2].

Alcohol distilleries are rated as one of the 17 most polluting industries by the Government of India. An average molasses based distillery generates 15 l of spent wash per litre of alcohol produced [3]. Distillery effluent is characterized by extremely high chemical oxygen demand (COD) (80–100 kg/m^3) and biochemical oxygen demand (BOD) (40–50 kg/m^3), apart from low pH, strong odor and dark brown color [4]. Apart from high organic content, distillery wastewater also contains nutrients in the form of nitrogen (1660–4200 mg/l), phosphorus (225–3038 mg/l) and potassium (9600–17,475 mg/l) [5] that can lead to eutrophication of water bodies. Further, its dark color hinders photosynthesis by blocking sunlight and is therefore deleterious to aquatic life [6]. Joshi [7] indicated that land disposal of distillery effluent can lead to groundwater contamination.

Adequate treatment of these effluents is, therefore, essential before being discharged into water bodies. In addition to pollution, increasingly stringent environmental regulations are forcing distilleries to improve existing treatment methods and also explore alternative methods of effluent management. The regulatory agencies in India require the distillery units to meet the effluent discharge quality standards for release of the wastewater into surface waters (COD < 0.1 kg/m^3, BOD < 0.03 kg/m^3) and sewers (COD < 0.3 kg/m^3, BOD < 0.1 kg/m^3) [4].

The high organic content of molasses spent wash makes anaerobic treatment attractive in comparison to direct aerobic treatment. Therefore, bio-methanation is the primary treatment step and is often followed by two-stage aerobic treatment before discharge into a water body or on land for irrigation [8]. Sugarcane molasses spent-wash after biological treatment by both anaerobic and aerobic method can still have a BOD of 250–500 mg/l [9]. Also, even though biological treatment results in significant COD removal, the effluent still retains the dark color [10]. The color imparting melanoidins are barely affected by conventional biological treatment such as methane fermentation and the activated sludge process [11]. Still, few researchers have explored to treat bio-digester effluent (BDE) effluent using newer treatment methods [12].

Treatment by electrocoagulation (EC) has been practiced for the treatment of the variety of effluents. Compared with traditional flocculation and coagulation, EC has the advantage of removing small colloidal particles. Electric field applied during EC process sets

* Corresponding author. Tel.: +91 1332 285319; fax: +91 1332 276535/3560.
E-mail addresses: vimalcsr@yahoo.co.in (V.C. Srivastava), id_mall2000@yahoo.co.in (I.D. Mall).

0304-3894/$ – see front matter © 2008 Elsevier B.V. All rights reserved.
doi:10.1016/j.jhazmat.2008.10.041

Table 1
Characteristics of bio-digester effluent used for the study.

Characteristics	Value
COD (mg/l)	15,600
BOD (mg/l)	7200
Cl^- (g/l)	3.0
SO_4^{2-} (g/l)	4.23
Total solid (g/l)	34.1
Total dissolved solids (g/l)	2.29
pH	4.93
Color	Dark black

smaller colloidal particles in motion, thus, increasing the probability of their coagulation. Addition of excessive amount of coagulants can be avoided due to their in situ generation by electro-oxidation of a sacrificial anode. EC equipment is simple and easy to operate. Short reaction time and low sludge production are two other advantages of this technique.

EC has been used for the removal of COD and color from various synthetic and actual industrial effluents [13–20]. However, there are only a few studies on the electrochemical treatment of alcohol distillery wastewaters in the literature [19,20]. Vlyssides et al. [19] observed a maximum COD removal of 89% for an influent having COD of 72,000 mg/l in a laboratory scale pilot plant using Pt/TiO_2 anode in the presence of sodium chloride as supporting electrolyte. Manisankar et al. [20] researched the effect of halides in the EC treatment of distillery effluent using anodized graphite plate anodes and graphite cathodes. A maximum of 93.5% of BOD reduction, 85.2% of COD reduction and 98.0% absorbance reduction was observed in the presence of sodium chloride as supporting electrolyte. However, no study is reported in open literature for the treatment of BDE.

Response surface methodology (RSM) is a statistical based technique, commonly used to optimize and understand the performance of complex systems. RSM is a collection of mathematical and statistical techniques useful for developing, improving and optimizing processes and can be used to evaluate the relative significance of several affecting factors even in the presence of complex interactions.

The objective of the present study is to investigate the COD reduction of a BDE in a batch EC reactor using iron electrodes. Several parameters, namely current density (j), initial pH (pH_0), inter-electrode distance (g) and electrolysis time (t) were investigated for their effects on the COD removal efficiency.

2. Materials and methods

2.1. Effluent and its characterization

The BDE used for the present study was obtained from nearby distillery. The effluent was characterized for various parameters namely COD, BOD, total solids, total dissolved solids, sulphate, chloride, etc., as per standard method of analysis [21]. Further, the COD of treated effluent was also measured. The main characteristic of the effluent used for the present study is given in Table 1. The data reported in Table 1 are average of duplicate experiments with maximum deviation of ±5%. It may be noted that effluent was acidic in nature and the COD/BOD is 2.2 which shows that the effluent is recalcitrant in nature.

2.2. Reactor

The lab-scale batch experimental setup used for the EC studies is shown in Fig. 1. Experiments were carried out in a 1.5 l (108 mm × 108 mm × 130 mm) rectangular reactor made up of Perspex glass. Iron plates of thickness 2 mm were used as electrodes. Dimensions of electrodes were 100 cm × 80 cm; and area of electrodes dipped into the solution was 80 mm × 70 mm. The total effective surface area of each electrode was 112 cm^2; and a 5 cm gap was maintained between the bottom of the electrodes and the bottom of the cell to allowed easy stirring. The spacing between two electrodes in EC cell was varied from 1 to 3 cm. Magnetic stirrers were used to agitate the solution. The j was maintained constant by means of a precision digital direct current power supply (0–20 V, 0–5 A).

2.3. Experimental design

A 4 factor 5 level unblocked full central composite design has been used in the present study as the experimental design model. This model is orthogonal and rotatable, and has 16 cubic points, 6 axial points and 2 center points. A total of 23 experiments have been employed in this work to evaluate the individual and interactive effects of the four main independent parameters on the COD removal efficiency. Percentage COD removal has been taken as a response of the system (Y), while four process parameters, namely, j: 44.15–223.25 A/m^2; pH_0: 2–8; g: 1–3 cm; and t: 30–150 min, have been taken as input parameters. For statistical calculations, the levels for the four main variables X_i (X_1 (j), X_2 (pH_0), X_3 (g), X_4 (t)) were coded as x_i according to the following relationship

$$x_i = \frac{X_i - X_0}{\delta X} \quad (1)$$

where X_0 is value of the X_i at the centre point and δX presents the step change. The variables and levels of the design model are given in Table 2. The actual experimental design matrix is given in Table 3. Mongomery [22] has defined the statistical terms and their definitions.

To analyze a process or system including a response Y, where Y depends on the input factors $x_1, x_2, \ldots, x_k$, the relationship between the response and the input process parameters are described as

$$Y = f(x_1, x_2, \ldots, x_k) + \varepsilon \quad (2)$$

where f is the real response function its format being unknown, and ε is the residual error which describes the differentiation that can be included by the function f. The results were analyzed using the coefficient of determination (R^2), Pareto analysis of variance (ANOVA) and response plots.

A non-linear regression method was used to fit the second-order polynomial Eq. (2) to the experimental data and to identify the rel-

Table 2
Process parameters and their levels for EC treatment of bio-digester effluent using Central Composite Design.

Variable (unit)	Factors (x)	Level				
		−2	−1	0	1	2
Current density, j (A/m^2)	X_1	44.65	89.29	133.94	178.58	223.23
Initial pH, pH_0	X_2	2	3.5	5	6.5	8
Inter electrode distance, g (cm)	X_3	1	1	2	3	3
Time of electrolysis, t (min)	X_4	30	60	90	120	150

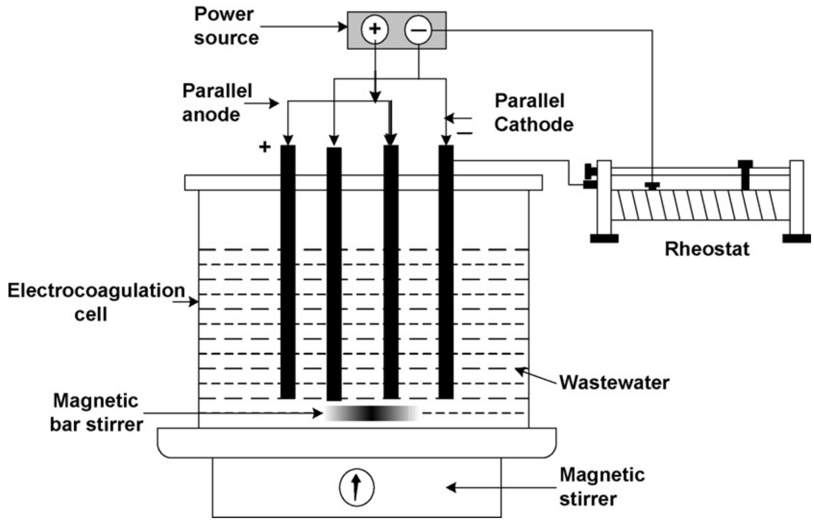

Fig. 1. Schematic diagram of the experimental setup used for the electrocoagulation study.

evant model terms using a statistical software, Design-expert V6. Considering all the linear terms, square terms and linear by linear interaction items, the quadratic response model can be described as

$$Y = \beta_0 + \sum \beta_i x_i + \sum \beta_{ii} x_{ii}^2 + \sum \beta_{ij} x_i x_j + \varepsilon \tag{3}$$

where β_0 is the offset term, β_i is the slope or linear effect of the input factor x_i, β_{ii} is the quadratic effect of input factor x_i and β_{ij} is the linear by linear interaction effect between the input factor x_i and x_j [23].

2.4. Experimental procedure

Each experimental run was carried out as per the conditions specified in the design matrix (Table 3). The experiments were performed on effluent of known initial COD (COD_0) and pH_0. The pH of the solutions was measured and adjusted by adding 0.1N NaOH or 0.1N H_2SO_4 solutions as per the run. The electrodes spacing was set appropriately as per design condition. At the beginning of a run, 1.5 l effluent was fed into the reactor, and power supply was switched on at $t = 0$. Current density was maintained constant during the run. Later samples were drawn from supernatant liquid and its final COD was measured.

The initial COD was determined before each experiment and percentage COD removal was calculated using the following relationship:

$$\text{percentage COD removal}\,(Y) = \frac{100(COD_0 - COD_t)}{COD_0} \tag{4}$$

where COD_0 is the initial COD (mg/l) and COD_t is the COD after t (min) of electrolysis time (mg/l).

2.5. Theory

EC process involves the generation of coagulants in situ by dissolving iron ions from iron electrodes. The in situ generation of iron

Table 3
Full factorial design used for the EC treatment of bio-digester effluent.

Std. order	j (X_1) (A/m^2)	pH_0 (X_2)	g (X_3) (cm)	t (X_4) (min)	% COD reduction	
					Y_{exp} (%)	Y_{pre} (%)
1	89.29	3.5	1	60	21.41	21.32
2	178.58	3.5	1	60	30.41	30.42
3	89.29	6.5	1	60	32.50	33.56
4	178.58	6.5	1	60	36.41	35.09
5	89.29	3.5	3	60	23.83	25.37
6	178.58	3.5	3	60	31.16	30.60
7	89.29	6.5	3	60	35.16	37.16
8	178.58	6.5	3	60	38.16	34.84
9	89.29	3.5	1	120	28.91	32.93
10	178.58	3.5	1	120	44.08	41.38
11	89.29	6.5	1	120	42.66	42.52
12	178.58	6.5	1	120	44.25	43.41
13	89.29	3.5	3	120	33.33	33.95
14	178.58	3.5	3	120	38.91	38.55
15	89.29	6.5	3	120	42.41	43.10
16	178.58	6.5	3	120	40.75	40.14
17	44.65	5	2	90	41.66	36.81
18	223.23	5	2	90	38.08	42.93
19	133.94	2	2	90	32.66	31.42
20	133.94	8	2	90	44.00	45.24
21	133.94	5	2	30	24.91	25.25
22	133.94	5	2	150	42.50	42.16
23	133.94	5	2	90	39.75	39.75

cations during EC process takes place at the anode, whereas at the cathode, typically H_2 production occurs.

Various reactions take place in the EC reactor with iron as electrode material [16,24–26].

- At iron anode

$$Fe \rightarrow Fe^{2+} + 2e^- \quad (5)$$

Also, in acidic pH, the electrode is attacked by H^+ and enhances its dissolution by following reaction:

$$Fe + 2H^+ \rightarrow Fe^{2+} + H_2 \quad (6)$$

Other reactions taking place in the vicinity of the anode are:
Under alkaline condition

$$Fe^{2+} + 2OH^- \rightarrow Fe(OH)_2 \quad (7)$$

Under acidic condition

$$Fe^{2+} + \frac{1}{4}O_2 + \frac{5}{2}H_2O \rightarrow Fe(OH)_3 + 2H^+ \quad (8)$$

Ferrous ions are oxidized to ferric ions by oxygen in the aqueous phase

$$Fe^{2+} + \frac{1}{4}O_2 + \frac{1}{2}H_2O \rightarrow Fe^{3+} + OH^- \quad (9)$$

The oxygen evolution reaction may also take place at anode and is represented as:

$$2H_2O \rightarrow O_2 + 4H^+ + 4e^- \quad (10)$$

- At cathode, following reduction reaction takes place.

$$2H_2O + 2e^- \rightarrow H_2 + 2OH^- \quad (11)$$

3. Results and discussions

3.1. Central composite design analysis

The most important parameters that affect the COD removal efficiency by EC are *j*, pH_0, *g*, and *t*. In order to study the combined effect of these factors, experiments were performed for different combinations of the physical parameters using statistically designed experiments. The range of values for the input variables is given in previous sections. The results of the *Y*(response) of COD removal by EC were measured according to design matrix and the measured responses are listed in Table 3.

A system with several variables is conducted primarily by some of the main effects and low order interactions and it may be assumed that the higher order interactions are small relative to the low order interactions. Therefore, in the present work only two-way interactions were considered. Linear, interactive, quadratic and cubic models were fitted to the experimental data to obtain the regression equations. To decide about the adequacy of various models to represent COD removal by EC, two different tests namely sequential model sum of squares and model summary statistics were carried out in the present study and the results are given in Table 4. Cubic model was found to be aliased and cannot be used for further modelling of experimental data. A model is aliased means that not enough experiments have been run to independently estimate all the terms for that model. Whenever, there are fewer independent points in the design than there are terms in the model, some parameters cannot be estimated independently. A model is aliased means that model is inappropriate for further investigation.

Sequential model sum of squares showed that the *p*-values were lower than 0.02 for quadratic and linear models (Table 4), therefore, both of these could be used for further study. However, model summary statistics showed that after excluding the cubic model which was aliased, quadratic model was found to have maximum "Adjusted R-Squared" and the "Predicted R-Squared" values. Therefore, quadratic model was chosen for further analysis.

Table 4
Adequacy of the models tested.

Source	Sum of squares	DF	Mean square	*F*-value	Prob > *F*	Remark
Sequential model sum of squares						
Mean	37643.2	1	37643.2			
Linear	772.28	4	193.07	14	<0.0001	Suggested
2FI	88.73	6	14.79	1.1	0.4016	
Quadratic	131.8	4	32.95	4.44	0.0177	Suggested
Cubic	94.62	7	13.52	41.67	0.0001	Aliased
Residual	1.95	6	0.32			
Total	38732.6	28	1383.31			
Source	**S.D.**	**Predicted R^2**	**Adjusted R^2**	**R^2**	**PRESS**	**Remark**
Model summary statistics						
Linear	3.71	0.7089	0.6583	0.5555	484.28	Suggested
2FI	3.67	0.7904	0.6671	0.3686	687.78	
Quadratic	2.73	0.9114	0.8159	0.2822	781.91	Suggested
Cubic	0.57	0.9982	0.992			Aliased

3.2. Fitting of second-order polynomial equation and statistical analysis

An empirical relationship expressed by a second-order polynomial equation with interaction terms was fitted between the experimental results obtained on the basis of central composite experimental design model and the input variables. The final equation obtained in terms of coded factors is given below:

$$\begin{aligned} Y = {} & 39.75 + 1.53X_1 + 3.46X_2 + 0.19X_3 + 4.23X_4 + 0.03X_1^2 \\ & - 0.36X_2^2 - 2.64X_3^2 - 1.51X_4^2 - 1.89X_1X_2 - 0.96X_1X_3 \\ & - 0.16X_1X_4 - 0.11X_2X_3 - 0.66X_2X_4 - 0.75X_3X_4 \end{aligned} \quad (12)$$

ANOVA is a statistical technique that subdivides the total variation in a set of data into component parts associated with specific sources of variation for the purpose of testing hypotheses on the parameters of the model [27]. The statistical significance of the ratio of mean square variation due to regression and mean square residual error was tested using ANOVA. The ANOVA for the second-order equation is presented in Table 5. The ANOVA indicated that the equation adequately represented the relationship between the response (the percentage COD removal) and the significant variables. According to ANOVA (Table 5), the Fisher *F*-values for all regressions were higher. The large value of *F* indicates that most of the variation in the response can be explained by the regression equation. The associated *p* value is used to estimate whether *F* is large enough to indicate statistical significance. *p*-values lower than 0.05 indicates that the model is statistically significant [28]. The ANOVA table also shows a term for residual error, which measures the amount of variation in the response data left unexplained by the model.

The ANOVA result for the COD removal by EC with Fe electrodes system shows *F*-value of 9.55, which implies that the terms in the model have a significant effect on the response. The model gives coefficient of determination (R^2) value of 0.9114 and an adjusted-R^2 value of 0.8159, which is high and advocates a high correlation between the observed and the predicted values. The probability *p* (∼0.0001) is less than 0.05. This indicates that the model terms are significant at 95% of probability level. Any factor or interaction of factors with $p < 0.05$ is significant.

Table 5
ANOVA of the second-order polynomial equation.

Source	Coefficient estimate	Sum of squares	DF	Mean square	F value	Prob > F	Remark
Model intercept	39.75	992.81	14	70.91	9.55	0.0001	Highly significant
X_1	1.53	56.30	1	56.30	7.58	0.0164	Significant
X_2	3.46	286.63	1	286.63	38.59	<0.0001	Highly significant
X_3	0.19	0.59	1	0.59	0.080	0.7820	
X_4	4.23	428.75	1	428.75	57.72	<0.0001	Highly significant
X_1^2	0.030	0.022	1	0.022	0.003	0.9578	
X_2^2	−0.36	3.02	1	3.02	0.41	0.5345	
X_3^2	−2.64	41.90	1	41.90	5.64	0.0336	Significant
X_4^2	−1.51	54.81	1	54.81	7.38	0.0176	Significant
$X_1 \times X_2$	−1.89	57.15	1	57.15	7.69	0.0158	Significant
$X_1 \times X_3$	−0.96	14.86	1	14.86	2.00	0.1807	
$X_1 \times X_4$	−0.16	0.41	1	0.41	0.055	0.8180	
$X_2 \times X_3$	−0.11	0.19	1	0.19	0.026	0.8742	
$X_2 \times X_4$	−0.66	7.00	1	7.00	0.94	0.3495	
$X_3 \times X_4$	−0.75	9.12	1	9.12	1.23	0.2879	
Residual		96.56	13	7.43			
Lack of fit		96.56	8	12.07			
Pure error		0.000	5	0.000			
Cor total		1089.37	27				

The ANOVA table obtained from the response surface quadratic model shows that j, pH_0, t, g^2, t^2, and $j \times pH_0$ are significant. The constant, which does not depend on any factors and interaction of factors, shows that the average COD removal of BDE by EC process using Fe electrodes is 39.75%, and that this average removal is independent of the factors set in the experiment. The ANOVA analysis indicates a linear relationship between Y and with that of j, pH_0 and t; and quadratic relationships between Y and with that of g, t, and the product of j and pH_0 ($j \times pH_0$). The analysis shows that the form of the model chosen to explain the relationship between the factors and the response is correct [29]. “Adeq Precision” measures the signal to noise ratio. A ratio greater than 4 is desirable. For the present study, signal to noise ratio was found to be 11.99, which indicates adequate signal. Therefore, quadratic model can be used to navigate the design space.

Data were also analyzed to check the normality of the residuals. A normal probability plot or a dot diagram of these residuals is shown in Fig. 2. The data points on this plot lie reasonably close to a straight line, lending support to the conclusion that j, pH_0, t, g^2, t^2, and $j \times pH_0$ are the only significant effects and that the underlying assumptions of the analysis are satisfied.

Fig. 3 shows the relationship between the actual and predicted values of Y for COD removal of BDE by EC process using Fe electrodes. It is seen in Fig. 3 that the developed model is adequate because the residuals for the prediction of each response are minimum, and the data points lie close to the diagonal line.

3.3. Effect of various parameters on maximum COD removal efficiency

The inferences obtained from the response surfaces to estimate maximum COD removal with respect to each variable, and each variable’s effect on COD removal efficiency are discussed below.

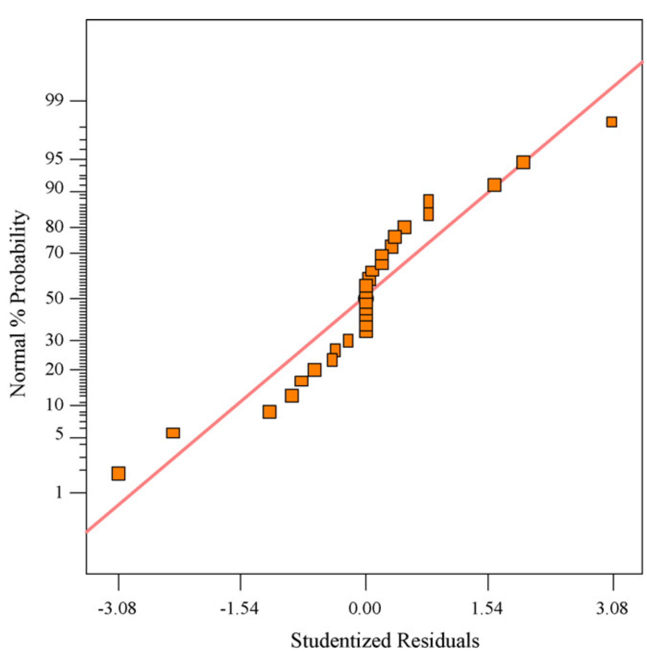

Fig. 2. Normal % probability versus residual error.

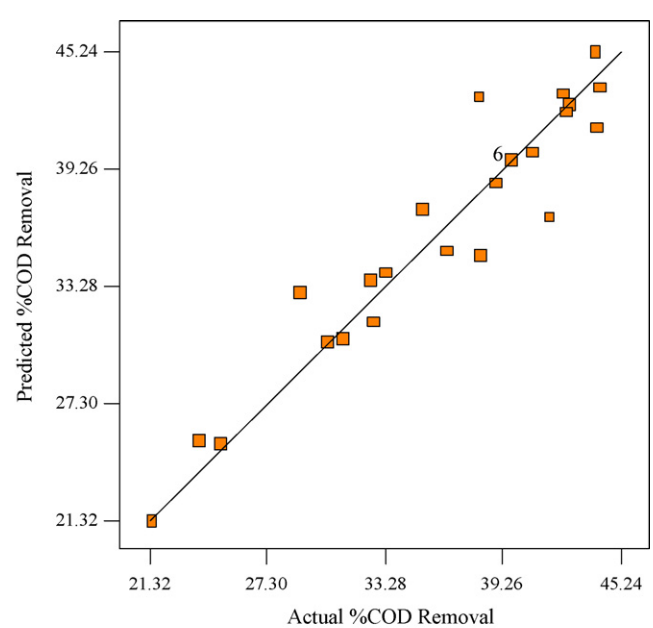

Fig. 3. Scatter diagram of predicted response versus actual response for the EC treatment of bio-digester effluent.

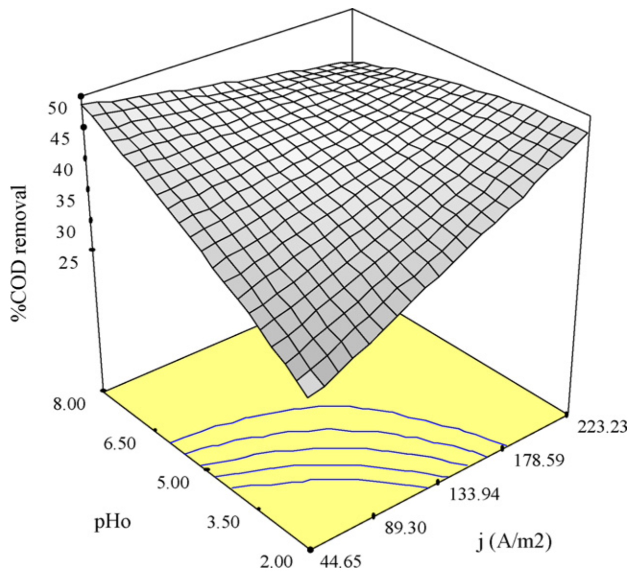

Fig. 4. 3D response surface graph for COD removal versus current density and initial pH for the EC treatment of bio-digester effluent.

3.3.1. Effect of current density (j) and initial pH (pH_0)

To study the effect of *j* and pH_0 on COD removal, experiments were carried out by varying *j* from 44.15 to 223.25 A/m^2 and under different pH_0 from 2 to 8. The results are plotted in Fig. 4 and Table 3. The COD removal efficiency was found to increase with an increase in *j* values at any value of pH_0.

Faraday's law describes the relationship between *j* and the amount of anode material that dissolves in the solution. It is given as

$$m = \frac{Mjt}{ZF} \quad (13)$$

where *m* is the theoretical amount of ion produced per unit surface area by current density *j* passed for a duration of time *t*. *Z* is the number of electrons involved in the oxidation/reduction reaction; for Fe, $Z = 2$. *M* is the atomic weight of anode material, for Fe, $M = 55.85$ g/mol; and *F* is the Faraday's constant (96,486 C/mol).

Generally it is known that COD removal increases with increasing iron dosages in chemical coagulation. In EC, therefore, COD removal is expected to be governed by the amount of hydrous oxides formed in the solution. According to Faraday's law, *m* is directly proportional to *j*. Therefore, COD removal by EC is governed by the formation of metal-hydrous ferric oxide complexes. It may be inferred from Fig. 4 that COD removal efficiency gets enhanced at higher *j* value. At higher *j*, elevated dissolution of electrode material (Faraday's law) with greater rate of formation of iron hydroxides results in higher COD removal efficiency via co-precipitation and sweep coagulation [24,30].

pH of the solution is of vital importance in the performance EC process. The metal ions generation takes place at the anode; hydrogen gas gets released at the cathode. The hydrogen gas helps in floatation of the flocculated particles out of the water. In an attempt to investigate the influence of pH_0 on the EC process, pH_0 of the effluent was varied in the range of 2–8 by adding 0.1N NaOH or 0.1N H_2SO_4 solution. The results illustrated in Fig. 2b demonstrate the COD removal efficiency at different pH_0. The results reveal that at $pH_0 \sim 8$, the COD removal efficiency was maximum. For $pH_0 < 8$, the protons in the solution get reduced to H_2, and thus, the proportion of hydroxide ion produced is less and consequently there is less COD removal efficiency [31].

Precipitation and adsorption are the two major interaction mechanism considered during EC process. Each of the mechanism is applicable at different pH ranges. At low pH values, metal species like Fe^{2+} generated at the anode bind to the anionic colloidal particles present in the BDE, thus, neutralizing their charge and reducing their solubility. This process of removal is termed precipitation. The adsorption mechanism operates at higher pH range (>6) and involves adsorption of organic substances on amorphous metal hydroxide precipitates [32,33]. In the present case, for pH < 6, the primary mechanism is charge neutralization by monomeric cationic iron species, while for higher pH, sweep coagulation with amorphous iron hydroxide explains the results [34].

3.3.2. Effect of electrolysis time (t) and electrode gap (g)

The effect of *g* and *t* on COD removal by EC under varying *g* (from 1 to 3 cm) and *t* (from 30 to 150 min) is plotted in Fig. 5. The COD removal efficiency depends directly on the concentration of ions produced by the electrodes which in-turn depends upon *t*. When the value of *t* increases, an increase occurs in concentration of iron ions and their hydroxide flocs. Consequently, an increase in the *t* increases the COD removal efficiency (Fig. 5).

The conductivity of the solution greatly affects the COD removal efficiency. The electrical conductivity is directly proportional to the distance between the two electrodes. As the distance between the anode and the cathode (*g*) increases, resistance (*R*) offered by the cell increases by the relation:

$$R = \frac{g}{KA} \quad (14)$$

where *K* is the cell specific conductance and *A* is electrode surface area. And, therefore, the current in the cell decreases at constant voltage by the relation: current = voltage/resistance. From Faraday's law, the amount of iron oxidized decreases as *g* increases, and thus, the COD removal efficiency generally decreases. Fig. 5 shows the effect of *g* on the COD removal efficiency during EC process. It may be seen that the COD removal efficiency generally remains constant with an increase in *g*. It seems that other factors namely *j*, pH_0 and *t* have over-riding effect on COD removal efficiency as compared to *g* as pointed in Section 3.2. Therefore, the effect of *g* of COD removal efficiency gets marginalized.

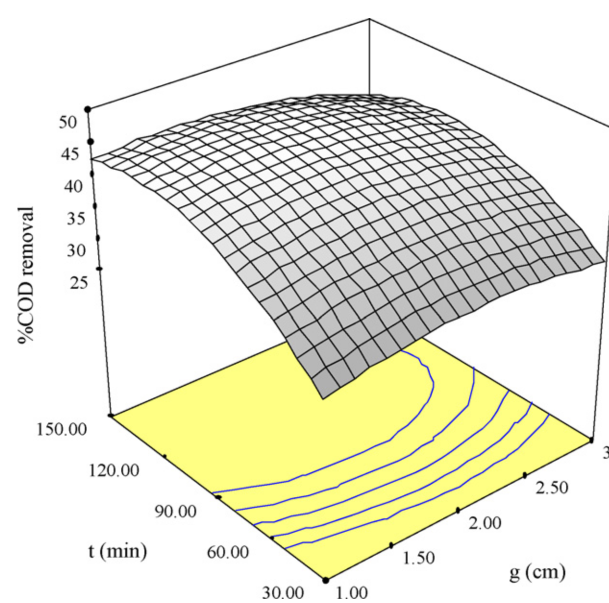

Fig. 5. 3D response surface graph for COD removal versus electrode gap and time for the EC treatment of bio-digester effluent.

Table 6
Optimum and confirmative values of process parameters for maximum COD removal efficiency.

Optimal levels of process parameters	Predicted optimal value with 95% confidence intervals (%)	Average of confirmation experiments (%)
j = 44.65 A/m^2 pH_0 8 g = 2 cm t = 120 min	41.21 < 51.69 < 62.18	50.5 ± 1.2

3.4. Selection of optimal levels and estimation of optimum response characteristics

The aim of the work is to removal maximum COD of BDE with minimum energy consumption. Table 6 summarizes the optimal level of various parameters obtained after examining the response curves and contour plots (not shown here) and Table 5. Regression analysis predicts that the experiments carried out at optimum conditions (j = 44.65 A/m^2, pH_0 8, g = 2 cm and t = 120 min) will give an average of 51.7% COD removal.

Three confirmation experiments were conducted at predicted optimal levels of the process parameters, and 50.5% average COD removal and 97.3% average color removal was observed at optimum conditions. The removal percentages obtained through confirmation experiments are within 95% of predicted values. It may be noted that that these optimal values are valid within the specified range of process parameters. Any extrapolation/interpolation should be confirmed through additional experiments.

To determine the electrode consumption, electrodes were removed from the EC reactor after EC. The anode consumption was found to be greater (1.361 g l^{-1} of solution) as compared to that of cathode (0.205 g l^{-1} of solution). Canizares et al. [34,35] carried out experiments to measure the chemical dissolution rate of iron electrodes at various pH. It was observed that the dissolution rate of iron was very less at basic pH and the dissolution rate increased significantly for acidic pHs. The dissolution rate was several orders of magnitude higher at acidic pH (≤2) as compared to that at basic or neutral pH. It was accompanied by evolution of hydrogen bubbles evolved from the sheet surface. This chemical dissolution of iron occurs via oxidation of iron electrode with simultaneous reduction of water to form hydrogen. Chemical dissolution of electrode can be represented by following reactions:

$$Fe + 2H_2O(l) \rightarrow Fe^{2+}(aq) + H_2(g) + 2OH^-(aq) \quad (15)$$

$$4Fe + 10H_2O(l) + O_2 \rightarrow 4Fe^{3+}(aq) + 4H_2(g) + 12OH^-(aq) \quad (16)$$

In each electrochemical cell, there is a pH profile between anode and cathode [35]. On the anode, the water oxidation process generates a high concentration of protons, resulting in a lower pH, whereas, water reduction at the cathode results in the formation of hydroxyl ions and, hence, in a higher pH. This means that, in the case of iron-based EC cells, on the anode surface is going to be more dissolved as compared to cathode.

3.5. Sludge disposal

Heating value of sludge as determined from bomb calorimeter was found to be 5.3 MJ/kg. This sludge can be utilized for making blended fuel briquettes with other organic fuels. This could be used as a fuel in the furnaces. The bottom ash obtained after its combustion can be blended with the cementious mixtures which is to be further used in construction purposes. Setting and leaching tests on the cementious mixtures have shown that the bottom ash can be incorporated into the cementious matrices to a great extent (75 wt.% of total solid) without the risks of an unacceptable delay of cement setting and an excessive heavy metals leachability from solidified products [36,37]. This method of EC residue disposal recovers energy from the residues as well it chemically fixes the iron and other toxic metals present in EC sludge.

4. Conclusion

The present study demonstrated the applicability of EC method for COD reduction of BDE. A central composite design was successfully employed for experimental design, analysis of results and optimization of the operating conditions for maximizing the COD removal. Analysis of variance showed a high coefficient of determination value (R^2 = 0.8547), thus, ensuring a satisfactory adjustment of the second-order regression model with the experimental data. Graphical response surface and contour plots were used to locate the optimum point. Maximum COD and color removal efficiency of 50.5% and 95.2%, respectively, was observed at optimum j, pH_0, g and t values of 44.65 A/m^2, 8, 2 cm and 120 min, respectively.

Acknowledgements

Authors (F.A.P., M.K., J.R.M.) are thankful to SRIC office, IIT Roorkee for providing financial support to undertake this research work. V.C.S. and I.D.M. are grateful to the Ministry of Human Resource and Development, Government of India, for financial assistance in the research work.

References

[1] K.A. Subramanian, S.K. Singal, M. Saxena, S. Singhal, Utilization of liquid biofuels in automotive diesel engines: an Indian perspective, Biomass Bioenergy 29 (1) (2005) 65–72.
[2] J. Uppal, Water utilization and effluent treatment in the Indian alcohol industry: an overview, in: P.K. Tewari (Ed.), Liquid Asset, Proceedings of the Indo-EU Workshop on Promoting Efficient Water Use in Agro-Based Industries, TERI Press, New Delhi, India, 2004, pp. 13–19.
[3] F.J. Beltran, J.F. Garcia-Araya, P.M. Alvarez, Wine distillery wastewater degradation 2. Improvement of aerobic biodegradation by means of an integrated chemical (ozone)-biological treatment, J. Agric. Food Chem. 47 (1999) 3919–3924.
[4] CPCB, Pollution Control Acts, Rules and Notifications Issued There Under, Central Pollution Control Board, Delhi, India, 2006.
[5] S. Mahimaraja, N.S. Bolan, Problems and prospects of agricultural use of distillery spentwash in India, in: SuperSoil 2004. 3rd Australian New Zealand Soils Conference, 5–9 December, University of Sydney, Australia, 2004.
[6] F. FitzGibbon, D. Singh, G. McMullan, R. Marchant, The effect of phenolic acids and molasses spentwash concentration on distillery wastewater remediation by fungi, Process Biochem. 33 (8) (1998) 799–803.
[7] H.C. Joshi, Bio-energy potential of distillery effluents, Energy News 3 (1999) 10–15.
[8] T. Nandy, S. Shastry, S.N. Kaul, Wastewater management in a cane molasses distillery involving bioresource recovery, J. Environ. Manag. 65 (2002) 25–38.
[9] I.D. Mall, V. Kumar, Removal of organic matter from distillery effluent using low cost adsorbent, Chemical Engineering World XXXII (7) (1997) 89–96.
[10] B. Inanc, F. Ciner, I. Ozturk, Color removal from fermentation industry effluents, Water Sci. Technol. 40 (1) (1999) 331–338.
[11] V.P. Migo, M. Matsumara, E.J.D. Rosario, H. Kataoka, Decolorization of molasses wastewater using an inorganic flocculant, J. Fermentation Bioeng. 75 (6) (1993) 438–442.
[12] P.K. Chaudhari, I.M. Mishra, S. Chand, Catalytic thermal pretreatment (catalytic thermolysis) of biodigester effluent of an alcohol distillery plant, Ind. Eng. Chem. Res. 44 (2005) 2518–2524.
[13] S. Mahesh, B. Prasad, I.D. Mall, I.M. Mishra, Electrochemical degradation of pulp and paper mill wastewater. Part 1. COD and color removal, Ind. Eng. Chem. Res. 45 (2006) 2830–2839.
[14] S. Mahesh, B. Prasad, I.D. Mall, I.M. Mishra, Electrochemical degradation of pulp and paper mill wastewater part II. Characterization and analysis of sludge, Ind. Eng. Chem. Res. 45 (2006) 5766–5774.
[15] X. Chen, G. Chen, L.Y. Po, Separation of pollutants from restaurant wastewater by electrocoagulation, Sep. Purif. Technol. 19 (2000) 65–76.
[16] K. Thella, B. Verma, V.C. Srivastava, K.K. Srivastava, Electrocoagulation study for the removal of arsenic and chromium from aqueous solution, J. Environ. Sci. Health Part A 43 (2008) 554–562.

[17] J.Q. Jiang, N. Graham, C. Andre, H.K. Geoff, N. Brandon, Laboratory study of electro-coagulation-floatation for water treatment, Water Res. 36 (2002) 4064–4078.
[18] R. Ahlawat, V.C. Srivastava, I.D. Mall, S. Sinha, Investigations on electrocoagulation treatment of cotton blue dye solutions using aluminum electrodes, CLEAN 36 (2008) 863–869.
[19] A.G. Vlyssides, C.J. Israilides, M. Loizidou, G. Karvouni, V. Mourafeti, Electrochemical treatment of vinasses from beet molasses, Water Sci. Technol. 36 (2/3) (1997) 271–278.
[20] P. Manisankar, C. Rani, S. Viswanathan, Effect of halides in the electrochemical treatment of distillery effluent, Chemosphere 57 (2004) 961–966.
[21] L.S. Cleceri, A.E. Greenberg, A.D. Eaton, Standard Methods For The Examination of Water and Wastewater, 20th ed., American Public Health Association, Washington, DC, 1998.
[22] D.C. Montgomery, Design and Analysis of Experiments, third ed., Wiley, New York, 1991.
[23] K.Y. Benyounis, A.G. Olabi, M.S.J. Hashmi, Effect of laser welding parameters on the heat input and weld-bead profile, J. Mater. Process. Technol. 164–165 (2005) 978–985.
[24] A.K. Golder, A.N. Samanta, S. Ray, Removal of trivalent chromium by electrocoagulation, Sep. Purif. Technol. 53 (2007) 33–41.
[25] C.F. Albert, Advanced Inorganic Chemistry: A Comprehensive Text, second ed., John Wiley, New York, 1966.
[26] F. Esmadi, J. Simm, Sorption of cobalt(II) by amorphous ferric hydroxide, Colloids Surf. 104 (1995) 265–270.
[27] L. Huiping, Z. Guoqun, N. Shanting, L. Yiguo, Technologic parameter optimization of gas quenching process using response surface method, Comput. Mater. Sci. 38 (3) (2007) 561–570.
[28] J. Segurola, N.S. Allen, M. Edge, A.M. Mahon, Design of eutectic photo initiator blends for UV/curable acrylated printing inks and coatings, Prog. Org. Coat. 37 (1999) 23–37.
[29] H.M. Kim, J.G. Kim, J.D. Cho, J.W. Hong, Optimization and characterization of UV-curable adhesives for optical communication by response surface methodology, Polym. Test. 22 (2003) 899–906.
[30] Z.R. Guo, G. Zhang, J. Fang, X. Dou, Enhanced chromium recovery from tanning wastewater, J. Cleaner Prod. 14 (1) (2006) 75–79.
[31] N. Modirshahla, M.A. Behnajady, S. Kooshaiian, Investigation of the effect of different electrode connections on the removal efficiency of tartrazine from aqueous solutions by electrocoagulation, Dyes Pigment 74 (2) (2007) 249–257.
[32] J. Duan, J. Gregory, Coagulation by hydrolysing metal salts, Adv. Colloid Inter. Sci. 100–102 (2003) 475–502.
[33] O.T. Can, M. Bayramoglu, M. Kobya, Decolorization of reactive dye solutions by electrocoagulation using aluminum electrodes, Ind. Eng. Chem. Res. 42 (2003) 3391–3396.
[34] P. Canizares, C. Jimenez, F. Martınez, C. Saez, M.A. Rodrigo, Study of the electrocoagulation process using aluminum and iron electrodes, Ind. Eng. Chem. Res. 46 (2007) 6189–6195.
[35] P. Canizares, F. Martınez, M. Carmona, J. Lobato, M.A. Rodrigo, Continuous electrocoagulation of synthetic colloid-polluted wastes, Ind. Eng. Chem. Res. 44 (2005) 8171–8177.
[36] T. Mangialardi, Disposal of MSWI fly ash through a combined washing-immobilisation process, J. Hazard. Mater. B98 (2003) 225–240.
[37] V.C. Srivastava, I.D. Mall, I.M. Mishra, Equilibrium modelling of single and binary adsorption of cadmium and nickel onto bagasse fly ash, Chem. Eng. J. 117 (2006) 79–91.